Non-centralised Control Strategies for Energy-efficient and Flexible Manufacturing Systems

Jenny L. Diaz C.[a], Carlos Ocampo-Martinez[a]

[a]*Automatic Control Department, Universitat Politècnica de Catalunya, Institut de Robòtica i Informàtica Industrial (CSIC-UPC), Llorens i Artigas 4-6, Planta 2, 08028 Barcelona, Spain (e-mail: {jenny.lorena.diaz, carlos.ocampo}@upc.edu).*

Abstract

The manufacturing industry is transforming towards smart, energy-efficient, and flexible manufacturing systems. In this regard, this work deals with the design of non-centralised control architectures to improve the energy efficiency of such systems and to promote their flexibility. Based on both the configuration of manufacturing systems and their coupling dynamics, these systems are divided into sub-systems, from which smaller control problems can be stated. Thus, control/management strategies can also be modularised to confer more flexibility to manufacturing systems. Then, by using suitable distributed optimisation techniques, and properly defining the consensus stages among the local controllers, the outputs from such controllers are optimally coordinated to minimise the total energy consumption of the whole system. The proposed control strategies are tested in simulation for a typical process line of automotive parts manufacturing industry, in which the main processing units are machine tools. Based on the obtained results, manufacturing systems and their control strategies could be suitably modularised using non-centralised control schemes, from which a closed-loop performance similar to its centralised counterpart can be achieved.

Keywords: Flexible manufacturing systems, Energy efficiency, Real-time energy management,Model predictive control, Non-centralised control, Distributed optimisation.

1. Introduction

The manufacturing industry is transforming towards Smart Manufacturing Systems (SMS) taking advantage of recent advances in sensing technology, connectivity, computer science, and data management. This transformation is known as Industry 4.0 and demands for smart, efficient, and flexible manufacturing systems. Besides, due to the changing demand and high customisation level of parts produced by the manufacturing industry, flexibility has become into one of the main goals of such transformation. Into the context of manufacturing industry, flexibility refers to the ability to respond quickly and efficiently to changing products design, production requirements, and market demands [1].

Although there is an increasing interest in SMS, few research works have focussed on the design of control strategies to improve the energy efficiency of such systems in real time while satisfying their flexibility and productivity requirements [2]. Regarding flexibility, researches have focused on designing modularised plants, process modelling, and process planning and scheduling to ensure the effectiveness of fulfilling the due dates and the optimal use of resources [1, 3]. However, the energy consumption has not been generally considered as a critical factor for the management of manufacturing systems and, most of the proposed approaches focus on maximising the production of parts that directly represent the revenue of a manufacturing plant. Besides, the few policies that focus directly on energy consumption are limited to an initial optimisation concerning production scheduling of existing plant devices [4, 5] or the use of rule-based controllers [6] designed according to the knowledge of the production processes.

The primary units of the discrete manufacturing industry are the machine tools, which refer to a set of machining devices that work sequentially to process a piece. However, in a real industry, machines are not isolated and interact with other machine tools and peripheral devices, which are responsible for supplying the required resources by the machines for their machining processes (e.g., milling, cutting, turning, grinding, drilling). It means, at high aggregation levels of manufacturing systems, its size and the complexity of the operational relationships among their constitutive elements increase. Thus, such complex and large-scale systems can be difficult to control/manage in order to minimise their energy consumption while satisfying their operational relationships and maintaining system productivity.

Therefore, to improve the energy efficiency of manufacturing systems by reducing energy consumption, large-scale manufacturing systems could be addressed as a set of many subsystems that interact with each other according to their process dynamics. Thus, the original control problem can be divided into smaller control problems, which could be solved separately and with a lower computational load [7]. Although the energy consumption dynamics can be easily separated for each sub-system, some process dynamics could involve several sub-systems resulting in coupled operational relationships. In this regard, the exchange of information between systems with coupled process dynamics is required to design control/management strategies that ensure the proper operation of manufacturing systems.

Optimisation-based control techniques have been useful for improving the energy efficiency of manufacturing systems, since from them the controller makes decisions to minimise the energy consumption of these systems, while the process dynamics related to the main functions of manufacturing systems (e.g. cutting or machining operations) can be added to the set of constraints of the optimisation problem to ensure the production of the parts. Thus, centralised control approaches based on optimisation can address coupling interactions by adding them into the set of constraints of the optimisation problem behind the controller design. In [6], a centralised control strategy based on Model Predictive Control (MPC) is proposed to minimise the energy consumption of a machine tool and its peripheral devices. However, such control schemes may require a high computational burden to achieve a solution when the size of manufacturing systems increases. Besides, centralised control approaches do not offer a high level of flexibility since the controller design should be fully updated if there is any change in operating conditions. To overcome such issues, the non-centralised control schemes have emerged as an alternative to control large-scale systems by dividing the whole system into sub-systems and the corresponding centralised control problem into smaller problems. These approaches can also contribute to the modularisation of the control systems allowing higher flexibility of manufacturing systems. In the related literature, different non-centralised control schemes have been proposed based on the communication among the controllers and their control objectives [7]. Among them, there exist the completely decentralised structures, distributed control systems with exchanging of information, and hierarchical structures [8, 9, 10].

During the last decade, the design of non-centralized control strategies based on Multi-Agent Systems (MAS), Game Theory, and dynamic system partitioning have gained acceptance into the new era of smart systems [11, 12, 13, 14, 15]. Among them, MAS have been widely used in the field of manufacturing systems due to its inherent features of agility and adaptability that promote flexibility. However, due to the complexity and high computational burden required by these strategies, most of the proposed approaches in manufacturing industry are related to process planning and scheduling and production control and making-decision rather than energy efficiency of SMS [11]. In [16], an MAS approach is proposed to control the production of a process line in the automotive industry. In addition, a dynamic decision support framework based on a genetic algorithm and MAS is proposed to simulate and optimize the production scheduling of complex real production environments by taking into account different types of uncertainty factors in [17]. In the same way as MAS, the application of game theory into manufacturing systems is focused on automated process planning and scheduling. In [13] and [18], game theory-based strategies for cooperative and data-driven process planning and scheduling are proposed (e.g., Pareto strategy, Nash strategy and Stackelberg strategy), and different optimization algorithms such as particle swarm optimization (PSO), simulated annealing (SA) and genetic algorithm (GA) are implemented to solve the optimization problem behind the proposed strategy. Then, although these tools have demonstrated suitable results towards flexible and smart systems, allowing the design of control strategies in an autonomous and adaptive way, their performance quite depends on the data-driven and communication technologies available in industry environments [16, 11].

Thus, the main contribution of this work refers to a methodology for the design of modularised control strategies that satisfy the energy-efficient, production, and flexibility requirements for the new manufacturing industry. In this regard, non-centralised control architectures are proposed to minimise the energy consumption of manufacturing systems without affecting their productivity. The latter means, to manage manufacturing systems without affecting the processing times of machines while assuring the proper operation of machining processes. Therefore, manufacturing systems are divided into sub-systems taking into account their configuration and the coupled dynamics among them. Then, MPC-based controllers are designed for each subsystem to minimise their total energy consumption based on a prediction of their energy consumption dynamics and including their process dynamics as constraints. However, due to the coupled dynamics among sub-systems, a methodology for decoupling such subsystems by adding a new consensus variable and by redefining the coupled dynamics is proposed. Next, by using suitable methods to solve optimisation problems in a distributed manner, such as the Alternating Direction Method of Multipliers (ADMM), a way to determine the consensus among the local controllers with coupled dynamics is proposed. In this regard, local controllers are coordinated to satisfy operational constraints while minimising energy consumption of sub-systems involved. To this end, both cooperative and non-cooperative control architectures are considered. Finally, the proposed approaches are compared with their centralised counterpart regarding their closed-loop performance and the computational burden, with the aim to check the viability of the modularisation of control systems using non-centralised control architectures.

The remainder of the paper is organised as follows. The problem statement, which have been focused on discrete manufacturing industry, is presented in Section 2. Next, the proposed approach to minimise the energy consumption of discrete manufacturing systems by using non-centralised control architectures is introduced in Section 3. In the last section, the manner to get the consensus among local controllers and the stopping criteria for the proposed algorithm are also explained. Then, in Section 4, the case study to be analysed is presented, including a detail description of the operational constraints for a manufacturing process line. Afterwards, the simulation results obtained from the proposed approach are presented and discussed in Section 5. Finally, in Section 6, conclusions and future works based on the obtained results are drawn.

2. Problem Formulation

In the context of discrete manufacturing industry, a process line is a complex system including several machines M_i and peripheral devices P_j that work synchronously and logically up to getting a finished part, as shown in Figure 1. Machines in a process line correspond to a set of machining devices that are directly related to machining processes, while the peripheral devices are those devices that provide the resources required to machines for their proper operation [19]. It should be noted that when a peripheral device is shared among two or more machines of the process line is called *global* peripheral device, and when the device work only for the i-th machine in the line is known as *local* peripheral device of the machine.

Machines in a process line are characterised by a *periodic* behaviour according to the sequence of machining operations and the total time required to process a piece, which is called *operation cycle* and denoted by T_{M_i}. Since peripheral devices supply resources to machines in the process line, there exist several functional relationships between machines and such devices that determine the productivity of the process line. Ideally, machines in a process line should operate without interruptions. Thus, the required resources for machining operations performed at every machine should be supplied at the proper instants and in the appropriate quantity to guarantee their continuous operation. In this regard, the activation instant and activation level of peripheral devices should be determined to satisfy the operational relationships while minimising the energy consumption of the whole process line.

Due to the operational relationships among machines and peripheral devices, manufacturing systems exhibit strong coupling dynamics that must be satisfied to guarantee the proper operation of the machine. According to Figure 1, coupling dynamics refer to the cases in which there exist multiple providers to one machine or when the resources should be shared among different machines. In both cases, it must be guaranteed that the required resource is supplied at the proper time instants and quantity according to the machining sequence of each machine. Besides, it is necessary to ensure that peripheral systems have the capacity enough to provide resources during the operation of the machines. Then, considering a fixed number of machines and peripheral devices in the process line, their activation sequences can be defined as

$$\mathbf{\Lambda_{M_i}}(k) = \{u_{M_{i,1}}(k), u_{M_{i,2}}(k), \ldots, u_{M_{i,m}}(k)\}, \tag{1a}$$

$$\mathbf{\Lambda_{P}}(k) = \{u_{P_1}(k), u_{P_2}(k), \cdots, u_{P_n}(k)\}, \tag{1b}$$

$\forall i = 1, 2, \cdots, p$, being $k \in \mathbb{Z}_{\geq 0}$ the discrete-time index and, $m = |\mathbf{\Lambda_{M_i}}|$ and $n = |\mathbf{\Lambda_P}|$ the total number of machining devices of the i-th machine and the number of peripheral devices in the process line, respectively. Usually, the activation signals of both machining devices and peripheral devices are constrained to $u_{M_{i,d}}(k) \in \{0, 1\}$, $d \in \mathcal{D} \triangleq \{1, 2, \cdots, m\}$, and $u_{P_j}(k) \in \{0, 1\}$, $j \in \mathcal{J} \triangleq \{1, 2, \cdots, n\}$. However, for the cases in which the activation load of devices can be modulated, the activation signal will be constrained to $u_{M_{i,d}}, u_{P_j} \in \mathbb{Z}_{\geq 0}$.

It is worth noting that $\mathbf{\Lambda_{M_i}}$ along T_{M_i} corresponds to the machining sequence of the i-th machine, which refers to all machining operations performed in such machine to process a piece. Since these operations are repeated every time a new piece arrives at the machine, every machine in the process line has a periodic behaviour that will be constant over time. Conversely, $\mathbf{\Lambda_P}$ could or could not exhibit a periodic behaviour that matches or not with some T_{M_i} for the machines in the process line. Then, the control objective is defined as the minimisation of the integral of the total energy consumption profile along a fixed period T, i.e.,

$$J(k) = \sum_{k=1}^{T} \left[\underbrace{\left(\sum_{i=1}^{p} S_{M_i}(k) \right) + \left(\sum_{j=1}^{n} S_{P_j}(k) \right)}_{S(k)} \right] \Delta k, \tag{2}$$

being $S \in \mathbb{R}$ the total energy consumption for the whole process line, $\Delta k = (t_k - t_{k-1})$, and $S_{M_i} \in \mathbb{R}$ and $S_{P_j} \in \mathbb{R}$ the energy consumption of the machines and peripheral devices, respectively. Due to the periodic behaviour that characterises machine tools, T can be defined according to the values of T_{M_i} for the different machines in the process lines. According to (2), energy consumption models for both the machines and peripheral devices are required to compute S. Then, the control problem consists of determining the activation/deactivation sequences of peripheral devices u_{P_j} that minimises (2) without affecting the processing times and the machining operations performed by the machines.

3. Non-centralised Control Architectures for SMS

As mentioned in Section 1, non-centralised control architectures can be designed as completely decentralised structures or distributed control systems according to the communication among local controllers. Decentralised control architectures refer to those controllers that are designed to operate in a completely independent fashion. It means that there is no communication among the local controllers designed for each sub-system. Such approaches are based on the assumption that the interactions among sub-systems are weak [20, 21]. However, due to the limited closed-loop performance of decentralised control systems given the lack of communication or information exchange among the local controllers, distributed control architectures have been deeply studied since they allow communication among the controllers to coordinate their actions [20].

Thus, in order to face the flexibility and modularity challenges of the new era of the manufacturing industry, and to design control strategies that can be suitable for their implementation in real time, a distributed control architecture based on MPC is proposed in this section assuming that the sub-systems have strong coupling dynamics between them. It is worth noting that the control strategy presented in this section is based on the non-cooperative case because it generally involves a lower computational burden. However, the modifications required to consider the cooperative case are presented and explained in Section 5.

First, taking advantage of the classification of manufacturing systems as machining and peripheral devices, the following assumption is established to avoid affecting the system productivity of the such systems.

Assumption 1. *The machining sequence of each machine, i.e.,* $\mathbf{\Lambda_{M_i}}$ *along* T_{M_i}, *is known and, hence, its associated apparent*

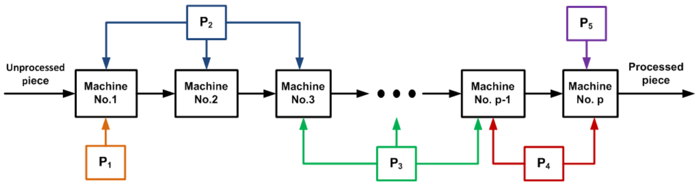

Figure 1: n-stage serial process line with its corresponding peripheral devices.

power consumption, $\beta_i \triangleq \sum_{k=1}^{T_{M_i}} S_{M_i}(\mathbf{\Lambda}_{\mathbf{M_i}}(k))$*, will be also known and periodic over time.* □

It should be noted that in the case Assumption 1 is not considered, the activation sequence for the machining devices could also be considered as a decision variable and, then, the time to process a piece by a machine and its productivity could be modified. Thus, taking into account that in a real manufacturing plant the sequence of machining devices is usually designed and optimised offline, if $\mathbf{\Lambda}_{\mathbf{M_i}}$ along T_{M_i} remains fixed and constant over time and only u_{P_j} is modified, the processing time of each machine remains the same and the machine can process the same number of pieces as when the control strategy is not implemented. Besides, including operational relationships between machines and peripheral devices into the controller design, the optimal operation of such machines could be guaranteed. In this regard, the activation of u_{P_j} will depend on the current energy consumption of the whole process line, the operational relationships between machines and peripheral devices, and the physical constraints of peripheral systems.

In a process line level, the functional relationships between machines and peripheral devices could be quite complex due to some peripheral devices can be shared among two or more machines or supply the same resource provided by another global peripheral device to a particular machine. In these cases, a consensus for the management of such devices should be established to guarantee the satisfaction of the operating constraints among the constitutive elements of the process line. Thus, according to the process line configuration and the coupled dynamics among machines and peripheral devices, manufacturing systems are divided into sub-systems, and the control problem is also split into smaller control problems, one for each subsystem. It means (2) is now given by

$$J(k) = \sum_{l=1}^{L} J^l(k), \tag{3}$$

being J^l the local cost function for the l-th sub-system defined as in (2) but considering only the energy consumption of the machines and devices related to such a sub-system. Then, local controllers are designed for each sub-system using J^l. Thus, considering a prediction horizon H_p, the activation sequence of peripheral devices for each local controller is given by[1]

$$\mathbf{\Gamma_P}^l(k) \triangleq \{\mathbf{\Lambda_P}^l(k|k), \dots, \mathbf{\Lambda_P}^l(k + H_p - 1|k)\}, \tag{4}$$

and each local controller l is based on the following open-loop optimisation problem

$$\min_{\mathbf{\Gamma_P}^l(k)} \quad J^l(k) \tag{5a}$$

subject to

$$\xi_h^l(k+1+r|k) = f_h^l\left(\xi_h^l(k+r|k), \mathbf{\Lambda}_{\mathbf{M_i}}{}^l(k+r|k), u_j^l(k+r|k)\right), \tag{5b}$$
$$S_h^l(k+r|k) = g_h^l\left(\xi_h^l(k+r|k)\right), \tag{5c}$$
$$Q_j^l(k+1+r|k) = q_j^l\left(Q_j^l(k+r|k), u_j^l(k+r|k), \mathbf{\Lambda}_{\mathbf{M_i}}{}^l(k+r|k)\right), \tag{5d}$$
$$m_{M_i}(k+r|k) = \varepsilon_{u_{P_j}}\, u_{P_j}^l(k+r|k) + \varepsilon_{u_{P_s}}\, u_{P_s}^b(k+r|k), \tag{5e}$$
$$u_j^l(k+r|k) \in \{n_1, n_2, \cdots, n_p^l\}, \tag{5f}$$
$$Q_j^l(k+r|k) \in \left[\overline{Q}_j^l,\ \underline{Q}_j^l\right], \tag{5g}$$

$\forall r = 0, 1, \dots, H_p - 1$, with i and j the indices for the machines and peripheral devices involved in the l-th sub-system, respectively. Moreover, b refers to the index for the other sub-systems with coupled dynamics to the l-th sub-system and the index s refers to the index of the peripheral devices involved in the b-th sub-system. It should be noted that (5b) and (5c) correspond to the energy consumption model of the h-th element (either M_i or P_j) in the l-th sub-system. Besides, (5d) refers to the operational relationships among the machines and devices involved in the l-th sub-system, while (5e) is related to the coupled dynamics among the l-th and b-th sub-systems. Thus, (5e) refers to the mass flow balance for a particular resource required by the i-th machine m_{M_i} during the machining operations. In (5e), values for $\varepsilon_{u_{P_j}}$ refer to the flow provided by each u_{P_j} when is turned on. In addition, expressions (5f) and (5g) refer to the range constraints for the decision variables and the operating ranges for the processes variables Q_j^l related to the operation of peripheral devices.

Then, to make the sub-systems with coupling dynamics separable and to use suitable algorithms for solving the problems in a distributed way, a new consensus variable z_j is introduced, (5e) is removed from the optimisation problem in (5), and a new balance constraint is defined as follows:

$$u_{P_j}^l(k+r|k) = z_j(k+r|k). \tag{6}$$

Replacing (5e) by (6), constraints in (5) are only related to the l-th sub-system and do not explicitly consider the interactions with the other sub-systems. Nonetheless, the variable z_j should contain the information about the real balance constraint in (5e) taking into account the amount of flow provided by the other sub-systems related to the same resource and machine.

[1] Here, $z(k+r|k)$ denotes the prediction of the variable z at time instant $k+r$ performed at k. The index r will cover the finite prediction window of length H_p.

Thereby, z_j should be suitably determined since it accounts for the compliment of (5e). The main advantage of this transformation is that since z_j could be considered as an external variable for every sub-system, the local control problem can be solved separately if z_j is known. In Section 3.1, a way to determine the values of z_j is presented.

Once the sub-systems and the related local control problems have been set, suitable optimisation algorithms should be selected to handle MPC problems in (5) distributively. Most of the algorithms proposed in the literature are iterative and require that some specific conditions are satisfied to converge to an optimal solution [22]. Some of the most used algorithms of this type are those based on the Lagrangian approach such as dual decomposition [23, 24], ADMM [22, 25], and the Accelerated Distributed Augmented Lagrangian (ADAL) [26, 27]. All these algorithms are based on the Lagrange dual theory, and the main difference among them concerns to the way they are used to decompose the augmented Lagrangian.

Regarding systems with coupled cost functions and constraints, the underlying idea behind the algorithms based on Lagrangian multipliers is to relax the coupled restrictions to make separable the optimisation problem. Thus, a Lagrange multiplier is added per each coupled constraint. In this work, the ADMM algorithm is employed to solve the optimisation problems in (5) in a distributed way. These algorithms were selected because they have the advantages of the dual decomposition algorithm, but do not require that the cost function was strictly convex due to the fact they define the augmented Lagrangian. Then, according to the ADMM algorithm [22], (6) is relaxed into the cost function by using of the Lagrange multipliers and, the augmented Lagrangian for each sub-problem (5) is defined as follows:

$$\mathcal{L}_\rho^l\left(\mathbf{\Gamma_P}^l, z, \lambda\right) = J^l(\cdot) + g_v(z) + (\lambda)^T\,(u^l_{P_j} - z_j) + \frac{\rho}{2}\|u^l_{P_j} - z_j\|_2^2, \quad (7)$$

with J^l the local cost function, $g_v(\cdot)$ a regularisation term for $z = [z_1, z_2, \cdots, z_j]$, and $\lambda = [\lambda_1, \cdots \lambda_j]$ the Lagrange multipliers for all the coupled constraints in the l-th sub-system. Then, (7) is the new cost function of the optimisation problem with two sets of decision variables, i.e., $\mathbf{\Lambda_P}^l$ and z, and with separable cost functions.

To solve (5), first, variables $\mathbf{\Lambda_P}^l$ are updated for each sub-system l considering an initial condition for z and λ. This step can be performed in parallel or in sequential way. Next, based on the updated values for $\mathbf{\Lambda_P}^l$, the consensus variable z is also updated. Finally, the Lagrange multipliers λ are updated by using the Gauss-Seidel method [22], and the procedure is repeated up to reach the convergence. These steps can be summarised as follows:

$$\mathbf{\Gamma_P}^l_{k+1} = \min_{\mathbf{\Gamma_P}^l}\left[J^l(\cdot) + \lambda_k^T\,(u^l_{P_j} - z_{j_k}) + \frac{\rho}{2}\|u^l_{P_j} - z_{j_k}\|_2^2\right], \quad (8a)$$

$$z_{k+1} = \min_z\left[g_v(z) + \sum_{l=1}^{b}\lambda_k^T\,(u^l_{P_{j_{k+1}}} - z_j) + \frac{\rho}{2}\|u^l_{P_{j_{k+1}}} - z_j\|_2^2\right], \quad (8b)$$

$$\lambda_{k+1} = \lambda_k + \rho\left(u^l_{P_{j_{k+1}}} - z_{j_{k+1}}\right), \quad (8c)$$

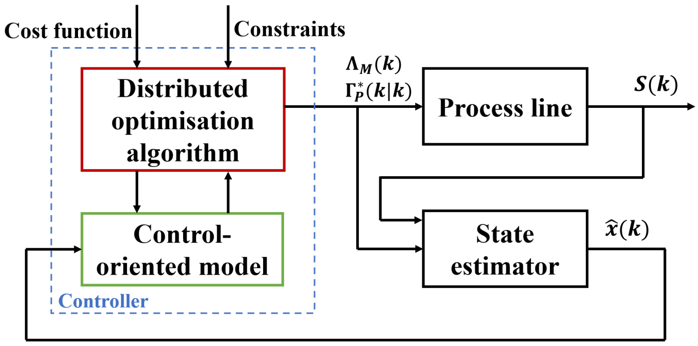

Figure 2: Proposed control scheme to minimise the energy consumption of a manufacturing process line.

with the subscript k indicating the current time step and $k+1$ the update at the next step. Thus, the local controllers for coupled sub-systems will be solved in a distributed way using the ADMM algorithm, while for the case of sub-systems with no coupled constraints will be solved in a decentralised way without information exchange with the other controllers.

Once convergence is achieved for the procedure in 8, there will be an optimal solution for the activation sequence of all peripheral devices in the process line defined by

$$\mathbf{\Gamma_P}^*(k) \triangleq \{\mathbf{\Lambda_P}^*(k|k), \ldots, \mathbf{\Lambda_P}^*(k + H_p - 1|k)\},$$

and, according to the receding horizon philosophy, $\mathbf{\Lambda_P}^*(k|k)$ is sent to the machine and peripheral devices discarding the rest of the optimal sequence from $(k+1|k)$ to $(k + H_p - 1|k)$. Then, the whole procedure is repeated for the next instant k, after measuring/estimating the information from the process line required by the controller. In Figure 2, the proposed closed-loop control scheme to determine $\mathbf{\Gamma_P}^*(k)$ along H_p is shown.

It should be noted that the optimisation problem in (8a) could be infeasible only if some of the constraints related to the process dynamics of peripheral devices are not satisfied. Therefore, due to the periodic behaviour of these systems, the length selected for H_p, and the execution time of the controller in a receding manner, it is possible to guarantee that the controller will be feasible at least for its next step of execution. In the next time step, the controller is run again and so on along the simulation horizon.

3.1. Consensus stage

Usually, the consensus problem based on the ADMM algorithms (i.e., (8b)) considers the regularisation term $g_v(\cdot)$ as averaging of the variable z concerning the number of sub-systems [22]. However, in this case, in addition to the balance constraint in (5e), the consensus stage should also penalise the energy consumption associated with the operation of peripheral devices. In this regard, $g_v(\cdot)$ in (8) should consider:

Balance constraint: The first term in $g_v(\cdot)$ penalises the error related to the balance constraint. Thus, at each instant k, such error is defined as

$$e_{M_i}(k) = \left(\varepsilon_{u_{P_j}}\, z_j(k) + \varepsilon_{u_{P_s}}\, z_s(k) - m_{M_i}(k)\right), \quad (9)$$

with j and s the indices related to the peripheral devices of the sub-systems l and b, which can supply the same resource to M_i. Thus, $\mathbf{E_{M_i}} = [e_{M_i}(1), e_{M_i}(2), \cdots, e_{M_i}(H_p)]^T$ is the error vector for (9) along H_p. In this case, the real constraint in (5e) is expressed in function of the consensus variable z, which is sent to the local controllers to guarantee the flow required by the machine. Then, $g_1(\cdot)$ is defined as follows:

$$g_1(z) = \mathbf{E_{M_i}}^T\, I_e\, \mathbf{E_{M_i}}, \tag{10}$$

being I_e the weighting matrix for (9) along H_p.

Energy consumption: According to the control objective in (2), the second term in $g_v(\cdot)$ accounts for the energy consumption associated to the operation of u_{P_j} but in terms of z, i.e.,

$$S_z(k) = \sum_{j=1}^{w} S_{z_j}(k), \tag{11}$$

being w the number of peripheral devices involved in (5e). Thus, the second term along H_p is defined as follows:

$$g_2(z) = \mathbf{S_z}^T\, I_{S_z}\, \mathbf{S_z}. \tag{12}$$

Finally, the whole regularisation term is given by

$$g_v(z) = \underbrace{\mathbf{E_{M_i}}^T\, I_e\, \mathbf{E_{M_i}}}_{g1} + \underbrace{\mathbf{S_z}^T\, I_{S_z}\, \mathbf{S_z}}_{g2}. \tag{13}$$

3.2. Stopping criteria

Based on the coupling constraints among the different subsystems, to determine the convergence of ADMM algorithm in (8), the following stopping criteria are defined:

Balance equation: It is defined to guarantee that the difference between the sum of the flows provided by all possible suppliers for M_i and the real flow required by the machine m_{M_i} will be less or equal to a tolerance value ϵ_1, i.e.,

$$\left(\sum_{j=1}^{p} \varepsilon_{u_{P_j}} u_{P_j}(k) \right) - m_{M_i}(k) \leq \epsilon_1. \tag{14}$$

Consensus constraint: It is defined to guarantee that each local controller takes into account the decisions made in the consensus stage. It is defined as follows:

$$u_{P_j}(k) - z_j(k) \leq \epsilon_2, \tag{15}$$

being ϵ_2 a value significantly small with respect to the magnitude of variables u_{P_j} and z_j. It should be noted that the stopping criteria are checked at each time instant k, for each time step along H_p.

4. Benchmark System

Consider a process line as shown in Figure 3, for which is assumed that all machine tools in the process line have different cycle time T_{M_i}. In addition, three global peripheral devices and one local device for M_1 are included to supply the resources required by the machines. In this case, it is assumed that devices P_{G_1} and P_{L_1} provide the flows of compressed air required by some of the machines in the line to clamp/unclamp of pieces during the operation of machines. Besides, P_{G_2} and P_{G_3} are responsible to supply the coolant flows required for all machines in the process line during machining operations. It is worth noting that both P_{G_1} and P_{L_1} can supply the airflow to M_1, while the rest of machines can only take the air from P_{G_1}. In the same way, both P_{G_2} and P_{G_3} can provide the coolant required by M_3 while P_{G_2} must also supply the coolant flows required by M_1 and M_2 while, in turn, P_{G_3} is responsible for the coolant demand of M_4. In this case it is supposed that M_4 does not require compressed air for its operation. It should be noted that the case study presented in Figure 3 has been designed based on a real case in a manufacturing plant.

According to Figure 3, in addition to the management of peripheral devices, the aperture of the valves related to machines with multiple suppliers, i.e., v_1-v_3 and v_2-v_4, should also be manipulated to ensure the supply of resources to machines. The other valves in the process line are not directly manipulated since it is assumed that they are opened/closed when required. Thus, the activation instants of peripheral devices and the aperture of valves refer to the decision variables, and their activation sequences are defined as

$$\mathbf{\Lambda_P}(k) = \{u_{G_1}(k), u_{G_2}(k), u_{G_3}(k), u_{L_1}(k)\}, \tag{16a}$$

$$\mathbf{\Lambda_V}(k) = \{\mathsf{v}_1(k), \mathsf{v}_2(k), \mathsf{v}_3(k), \mathsf{v}_4(k)\}. \tag{16b}$$

Based on both (5b) and (5d), energy consumption models and the operational relationships among machines and peripheral devices should be added into the optimisation problem in (5) to determine the optimal sequences of $\mathbf{\Lambda_P}$ and $\mathbf{\Lambda_V}$. In the following sections, it is presented how energy consumption models and operational relationships were determined.

4.1. Energy consumption models

Different approaches have been proposed for modelling manufacturing systems, such as phenomenological-based models, the Markov chains (MC), Petri Nets (PN), among others [28]. However, these approaches have been focused on modelling the production states of the machine rather than to model the energy consumption behaviour of such systems. Besides, they require a high computational load for control applications as well as the knowledge of a lot of variables/parameters that usually are difficult to measure/estimate in a manufacturing plant. Thus, since the complexity of manufacturing systems and their size, data-driven models, such as those obtained from the Subspace Identification (SI) methods, have gained attention into the manufacturing industry to model the specific energy consumption [29, 19].

The SI methods allow identifying the matrices of a state-space realisation of linear time-invariant (LTI) systems based on input-output data sets, which are convenient for estimation, control and prediction tasks [30]. These methods start from the idea that a set of measurements of n_u input signals ($n_u \geq 1$) and n_s output signals ($n_s \geq 1$) are related through an N-order

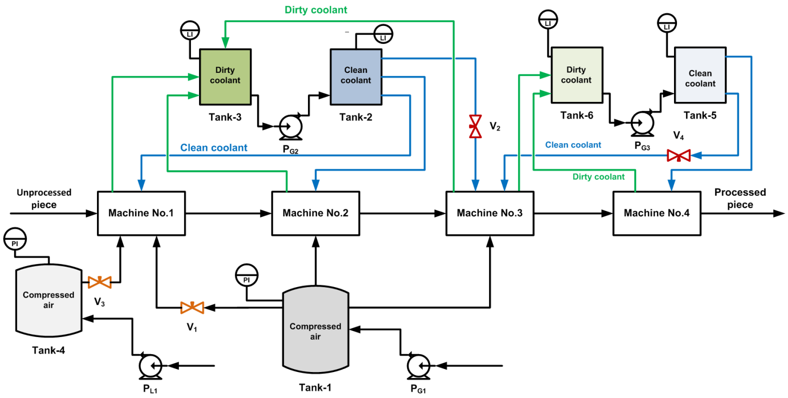

Figure 3: Four-stage serial process line with four peripheral devices.

Table 1: Model order and fitting percentage for the energy consumption models identified by SI methods.

Component	M_1	M_2	M_3	M_4	P_{G_1}	P_{L_1}	P_{G_2}	P_{G_3}
N	5	6	4	5	6	6	3	3
% fitting	96.27	96.76	96.85	95.32	98.82	97.83	94.22	94.22

state-space (unknown) realisation as follows:

$$\xi_h(k+1) = A\,\xi_h(k) + B\,\mathbf{\Lambda_h}(k), \tag{17a}$$

$$S_h(k) = C\,\xi_h(k) + D\,\mathbf{\Lambda_h}(k), \tag{17b}$$

being h the index for any machine or peripheral device, $\mathbf{\Lambda_h}$ the vector of input signals as in (16), S_h the instantaneous power consumption, and A, B, C and D the model matrices of suitable dimensions.

Then, to identify energy consumption models of machines in Figure 3, different sequences of $\mathbf{\Lambda_{M_i}}$ were designed, i.e., one sequence per each machine. Next, these sequences and different sequences of $\mathbf{\Lambda_P}$ were tested in a test bench that emulate the energy consumption of machine tools and their peripheral devices to obtain a rich range of their corresponding outputs S_{P_j} and S_{M_i}. Subsequently, the energy consumption models for the machines and the peripheral devices were identified by using the `n4sid` routine of the System Identification Toolbox™ provided by Matlab®. In this regard, different values of N were tested to identify the suitable matrices A, B, C, and D, which allow the highest fitting degree between the real and modelled outputs. In Table 1, the obtained results regarding the model order and the fitting percentage between the modelled and real outputs are presented for each one of the machines and peripheral devices. From these results, it can be concluded that the identified energy consumption models suitably represent the real energy consumption dynamics of both machines and peripheral devices.

In addition to the energy consumption of peripheral devices and machines, it was assumed that the valves related to the subsystem with coupled dynamics also imply an associated energy consumption. Thus, the energy consumption concerning valves is computed according to

$$S_{\mathsf{v}_j}(k) = \alpha_{\mathsf{v}_j}\,\mathsf{v}_j(k), \tag{18}$$

being α_{v_j} the constant energy consumption of the valve v_j.

4.2. Operational relationships

According to Figure 3, both P_{G_1} and P_{L_1} are associated to the supply system of compressed air, which will be used for clamping pieces during the whole machining sequence. Besides, it is assumed that both P_{G_1} and P_{L_1} have a nominal energy consumption whenever the device is turned on. In this regard, the process dynamics related to the operation of both P_{G_1} and P_{L_1} correspond to the mass and pressure dynamics inside the respective tanks, which are defined as follows:

$$M_{T_1}(k+1) = M_{T_1}(k) + \tau_s\,\sigma_{T_1}(k), \tag{19a}$$

$$\sigma_{T_1}(k) = m_{in,G_1} u_{G_1}(k) - m_{G_1\to M_1}(k) - \sum_{i=2}^{3} m_{a,M_i}(k), \tag{19b}$$

$$P_{T_1}(k) = \frac{M_{T_1}(k)\,R\,T}{V_{T_1}\,W_a}, \tag{19c}$$

being $u_{G_1} \in \{0,1\}$ the activation signal for P_{G_1}, m_{a,M_i} the air consumption from machine M_i, m_{in,G_1} the air flow pumped by P_{G_1} towards the tank T_1, and, R, T, V_{T_1} and W_a the gas constant, air temperature, volume of T_1, and the molecular weight, respectively. A set of equations similar to (19) can be defined for P_{L_1} regards Tank 4 taking into account their inputs and outlets. In this regard, $u_{L_1} \in \{0,1\}$ refer to the activation signal for P_{L_1}, m_{in,L_1} is the air flow pumped by P_{L_1} towards the tank T_4, and, $\sigma_{T_4}(k) = m_{in,L_1}\,u_{L_1}(k) - m_{L_1\to M_1}(k)$. Since both P_{G_1} and P_{L_1} can provide the airflow required by M_1, the following equation should be satisfied:

$$m_{a,M_1}(k) = m_{G_1\to M_1}(k) + m_{L_1\to M_1}(k), \tag{20}$$

with $m_{G_1\to M_1}(k) = \varepsilon_{\mathsf{v}_1}\,\mathsf{v}_1(k)$, $m_{L_1\to M_1}(k) = \varepsilon_{\mathsf{v}_3}\,\mathsf{v}_3(k)$, and being v_1 and v_3 the valve aperture to allow the flow from P_{G_1} and P_{L_1}, respectively. Moreover, the pressure P_{T_1} and P_{T_4} must remain inside an operational range to avoid damage in the peripheral systems and to ensure that there will be enough capacity to provide the resources during the operation of machines. Thus, $\underline{P}_{T_1} \le P_{T_1}(k) \le \overline{P}_{T_1}$ (and $\underline{P}_{T_4} \le P_{T_4}(k) \le \overline{P}_{T_4}$) should be satisfied, with $\underline{P}_{T_i}$ and $\overline{P}_{T_i}$ the lower and upper bounds for each tank.

On the other hand, both P_{G_2} and P_{G_3} are related to a coolant supply systems in the process line, for which their activations could be modulated to different energy consumption levels. In these cases, the dynamics of interest refer to the level changes in the tanks related to both P_{G_2} and P_{G_3}, which are given by

$$L_2(k+1) = L_2(k) + \tau_s\, \gamma_{T_2}(k)\left(\frac{1}{\rho_c\, A_{T_2}}\right), \tag{21a}$$

$$\gamma_{T_2}(k) = m_{c,G_2}(k) - \sum_{i=1}^{2} m_{cc,M_i}(k) - m_{cc,G_2\to M_3}(k), \tag{21b}$$

$$L_3(k+1) = L_3(k) + \tau_s\, \theta_{T_3}(k)\left(\frac{1}{\rho_c\, A_{T_3}}\right), \tag{21c}$$

$$\theta_{T_3}(k) = \sum_{i=1}^{3} m_{dc,M_i}(k) - m_{c,G_2}(k), \tag{21d}$$

with m_{c,G_2} given by

$$m_{c,G_2}(k) = \frac{\eta\, \rho_c\, u_{G_2}(k)}{P_{in,G_2}(k) + \rho_c\, h_{f_{G_2,1\to 2}}(k) - P_{out,G_2}(k)}, \tag{22}$$

being $u_{G_2} \in \{0, 100, 120, 140\}$ the activation signal of P_{G_2}. Similarly, level dynamics can be defined for Tanks 5 and 6 regarding the operations of P_{G_3} taking into account the inputs and outputs for each tank. Besides, it should be noted that for P_{G_3}, the activation signal is constrained to $u_{G_3} \in \{0, 70, 140\}$.

In (21), $m_{cc,j\to M_i}$ refers to the coolant flow supplied by the j-device to M_i, and $m_{dc_{M_i}}$ is the flow of dirty coolant recovered from machines. In addition, $P_{in,j}$ and $P_{out,j}$ correspond to the input and output pressure in the pipe system that connects the clean and dirty coolant tanks, while, ρ_c, η, ω and $h_{f_{j,1\to 2}}$ are the coolant density, the pump efficiency, the specific work per time unit and the energy losses by friction, respectively. Then, to satisfy the demand of coolant required by M_3, the following constraint should be satisfied:

$$m_{cc,M_3}(k) = m_{cc,G_2\to M_3}(k) + m_{cc,G_3\to M_3}(k), \tag{23}$$

with $m_{cc,G_2\to M_3}(k) = \varepsilon_{\mathsf{v}_2}\, \mathsf{v}_2(k)$, $m_{cc,G_4\to M_3}(k) = \varepsilon_{\mathsf{v}_4}\, \mathsf{v}_4(k)$, and being v_2 and v_4 the valve aperture related to each coolant supply system. Besides, the operational ranges for L_{T_i} must also be considered (5), i.e., $\underline{L}_{T_i} \leq L_{T_i}(k) \leq \overline{L}_{T_i}$.

Based on the real operation of machine tools, in Figures 4 and 5 are presented the sequences for the resources consumption of both compressed air m_{a,M_i} and coolant m_{cc,M_i} from each machine according to their cycle times T_{M_i}. Such sequences represent the demand for resources from machines to process a piece. Thus, these sequences are also periodic over time and repeated when a new piece arrives the machine. Moreover, it is worth noting that (20) and (23) refer to the coupled dynamics for the machines M_1 and M_3, respectively.

4.3. System partitioning

According to Figure 3, both M_1 and M_3 have multiple providers, while P_{G_1} and P_{G_2} must supply resources to two or more machines in the process line. In these cases, the controller should decide which peripheral device is more suitable to supply this demand taking into account the consumption from the other machines and the current levels in the supply systems. Besides, the maximum flow that can be provided when the valves are entirely opened must be considered to get a consensus among the values when more than one device is needed to supply resources to one machine.

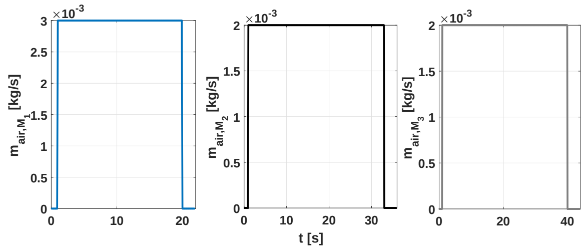

Figure 4: Sequences for the air consumption from machines in the four-stage process line along T_{M_i}.

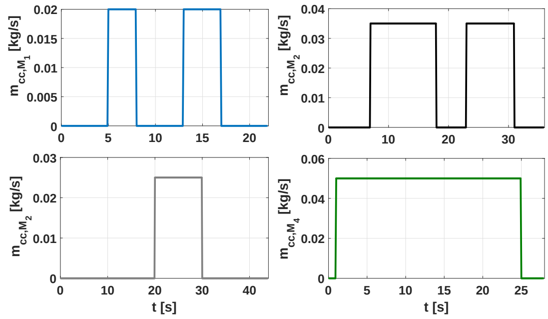

Figure 5: Sequences for the coolant consumption from machines in the four-stage process line along T_{M_i}.

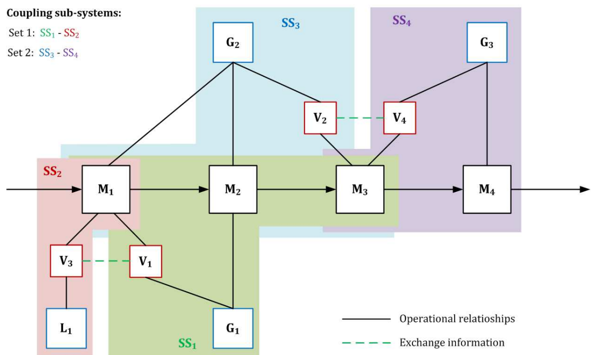

Figure 6: Proposed sub-systems division for the four-stage serial process line in Figure 3.

Based on the process line configuration and coupled dynamics among the different machines and peripheral devices, the process line is divided into four sub-systems, as shown in Figure 6. Such a system partitioning is proposed with the aim to increase the system flexibility by reducing the number of coupled sub-system and, therefore, the communication among controllers. However, other sub-systems could be defined depending on the information exchange among the local controllers, the optimisation algorithm to be used, and the computational capacity to solve such algorithms.

Sub-system 1 (SS_1) is formed by the machines M_1, M_2, M_3, the device P_{G_1}, and the valve v_1. This sub-system deals with the supply of compressed air to most of the machines in the process line. However, M_1 has also as a local supplier, i.e., L_1. Thus, the second sub-system (SS_2) is formed by P_{L_1}, v_3 and only M_1. From these two sub-systems, communication is required to supply the exact flow of compressed air required by M_1 as in (20).

The third (SS_3) and fourth (SS_4) sub-systems were defined concerning the supply system of coolant to machines in the process line. Thus, SS_3 consists of the machines M_1, M_2, and M_3, P_{G_2} and v_2. This sub-system represents the main coolant-supply system of the process line. Then, the sub-system SS_4 concerns to machines M_3 and M_4, the device P_{G_3} and v_4. This sub-system is responsible for satisfying the requirements of M_4 and should also coordinate with SS_3 to supply the coolant demand of M_3. Although there exists clear operational relationships among SS_1 and SS_2, and SS_3 and SS_4, there is not coupling dynamics among the supply systems of compressed air and coolant. That means, it is not necessary to establish communication among the supply systems of different resources to machines.

Table 2: Physical dimensions and parameters for the supply systems of compressed air and coolant.

Parameter	Value	Units	Parameter	Value	Units
Physical dimensions for the supply systems					
T_{M_1}	22	s	T_{M_2}	36	s
T_{M_3}	44	s	T_{M_4}	28	s
V_{T_1}	0.015	m^3	V_{T_4}	0.01	m^3
A_{T_2}	0.015	m^2	A_{T_3}	0.015	m^2
A_{T_5}	0.015	m^2	A_{T_6}	0.015	m^2
T_{air}	25	°C	R	8.1314	$\frac{\mathrm{J}}{\mathrm{Kmol}}$
W_{air}	28.966	$\frac{\mathrm{g}}{\mathrm{mol}}$	ΔP_{filter}	10000	Pa
P_{atm}	101325	Pa	η	0.95	–
ρ_c	1042.5	$\frac{\mathrm{kg}}{\mathrm{m}^3}$	$h_{1\to 2}$	0.12	$\frac{\mathrm{m}^2}{\mathrm{s}^2}$
$m_{in,1}$	0.006	$\frac{\mathrm{kg}}{\mathrm{s}}$	$m_{in,3}$	0.004	$\frac{\mathrm{kg}}{\mathrm{s}}$
α_{v_1}	2.5	VA	α_{v_3}	2.5	VA
α_{v_2}	2.25	VA	α_{v_4}	2.75	VA
$\varepsilon_{\mathsf{v}_1}$	1.5×10^{-5}	–	$\varepsilon_{\mathsf{v}_3}$	3.0×10^{-5}	–
$\varepsilon_{\mathsf{v}_2}$	2.5×10^{-4}	–	$\varepsilon_{\mathsf{v}_4}$	2.5×10^{-4}	–
$\underline{P}_{T_1}$	300	kPa	$\overline{P}_{T_1}$	750	kPa
$\underline{P}_{T_4}$	300	kPa	$\overline{P}_{T_4}$	750	kPa
$\underline{L}_{T_2}$	0.3	m	$\overline{L}_{T_2}$	0.6	m
$\underline{L}_{T_3}$	0.4	m	$\overline{L}_{T_3}$	0.7	m
$\underline{L}_{T_5}$	0.3	m	$\overline{L}_{T_5}$	0.6	m
$\underline{L}_{T_6}$	0.4	m	$\overline{L}_{T_6}$	0.7	m
ADMM algorithm					
ρ^1	0.1	–	ρ^2	0.01	–
λ_0^1	$[1, 1, \cdots, 1] \in \mathbb{R}^{H_p}$	–	λ_0^2	$[1, 1, \cdots, 1] \in \mathbb{R}^{H_p}$	–
z_j^0	$[0, 0, \cdots, 0] \in \mathbb{R}^{H_p}$	–	ϵ_1	1×10^{-4}	–
ϵ_2	0.5	–	ϵ_J	1×10^{2}	–

5. Simulation results

In this section, a comparison among the proposed non-centralised control strategies (cooperative and non-cooperative cases) and its centralised counterpart is presented. Simulations were performed using an Intel Core i7-55000U 2.4 GHz processor with 8G RAM, and the simulation results were obtained in Matlab by using the software IBM ILOG CPLEX Optimisation Studio [31] integrated to YALMIP toolbox [32]. In the top of Table 2, the physical dimensions of supply systems, the energy consumption of valves, and the operating range for process variables related to the operation of peripheral devices are presented. Such parameters were set based on the real operation of peripheral devices in the process line.

Due to different cycles times of machines in the process line, simulations were performed considering $H_p = 22$ s, which corresponds to the shorter machine cycle for machines in the process line. The latter means that if the controller is executed every second, such a controller makes 22 decisions along H_p, and each decision is remained during 1 second. It is worth noting that $H_p = 22$ s was selected to reduce the number of decision variables in the optimisation problem and, therefore, the computational burden. Besides, no significant improvements were observed when the length of H_p was equal to the longer cycle time for the machines in the process line.

Then, based on the proposed approach, in Algorithm 1 the steps to solve the non-cooperative control architecture for the particular case study in Figure 3 are presented. Besides, the convergence parameters (ρ^l), the initial condition for the Lagrangian multipliers (λ_0^l), and the tolerance values established to run the ADMM algorithm are presented at the bottom of Table 2. These parameters were defined by a trial-and-error procedure up to find the parameters that allow reaching an optimal solution with the minor number of iterations. For the cooperative case, the local cost function was the same for all local controller, including the energy consumption of all elements of the process line. In addition, a new stopping criteria was added in Algorithm (1) to ensure that all local controllers converge to the same (approximate) value of the global cost function $J(\cdot)$, i.e., $|J_l(k) - J_r(k)| \leq \epsilon_J, \ \forall \ j \neq r$ with ϵ_J a small-enough tolerance value.

Based on the coupled dynamics in (20) and (23) for sub-systems $1-2$ and $3-4$, respectively, four new variables z_j were added and constrained to be equal to the corresponding valve aperture v_j. It means that for each local controller, $\mathsf{v}_j = z_j$ was added as a constraint, and (20) and (23) were removed from the optimisation problem. Then, taking into account that SS_1 and SS_2 have coupled dynamics but do not share operational relationships with SS_3 and SS_4, which are coupled among them, two consensus stages are required, one for SS_1 and SS_2 regarding M_1 and another for SS_3 and SS_4 regarding M_3. Thus, for each set of coupled subsystems, $g_v(\cdot)$ was defined according to (9) and (11) taking into account the number of peripheral devices involved. Besides, the weighting matrices, i.e., I_e and I_{S_v}, were set as $I_e = 1 \times 10^4 I_{H_p}$ for both consensus stages, and $I_{S_v}^{1-2} = 10 \ I_{H_p}$ and $I_{S_v}^{3-4} = 5 \times 10^3 \ I_{H_p}$ for the consensus among sub-systems $1-2$ and $3-4$, respectively. It should be noted that these weighting matrices were adjusted by using a trial-and-error procedure taking as reference the obtained results for the centralised control architecture. Differences among $I_{S_v}^{1-2}$ and $I_{S_v}^{3-4}$ refer to the fact v_1 and v_3 have the same energy consumption (i.e., $\alpha_{\mathsf{v}_1} = \alpha_{\mathsf{v}_3}$), while in the second coupled sub-systems v_4 has higher energy consumption than v_2. Thus, for the case of SS_3 and SS_4, the energy consumption term in (13) is quite relevant to determine the trade-off between peripheral devices that satisfy the balance constraint while minimising energy consumption. For SS_1 and SS_2, the energy consumption will be

Algorithm 1 Non-cooperative model predictive control.

1: Define $\mathbf{\Lambda_P}$ and $\mathbf{\Lambda_V}$ along H_p:

$$\mathbf{\Gamma}^l(k) \triangleq \{\mathbf{\Lambda_P}^l(k|k), \ldots, \mathbf{\Lambda_P}^l(k+H_p-1|k)\},$$
$$\mathbf{\Pi}^l(k) \triangleq \{\mathbf{\Lambda_V}^l(k|k), \ldots, \mathbf{\Lambda_V}^l(k+H_p-1|k)\}.$$

2: Initialise $z(k)$ and $\lambda(k)$ along H_p

3: **repeat** for each l

4: Broadcast $z(k)$ and $\lambda(k)$ among the coupled sub-systems

5: Solve

$$\bar{\mathbf{\Gamma}}^{\mathbf{l}}, \bar{\mathbf{\Pi}}^{\mathbf{l}} = \min_{\mathbf{\Gamma}^l(k), \mathbf{\Pi}^l(k)} \left[J^l(\cdot) + \lambda(k)^T \left(\mathsf{v}_j{}^l(k) - z_l(k)\right) + \frac{\rho}{2} \|\mathsf{v}_j{}^l(k) - z_j(k)\|_2^2 \right],$$

subject to

(5b), (5d), (5f), (5g)

6: Solve the consensus problem under $\bar{\mathbf{\Gamma}}^{\mathbf{l}}, \bar{\mathbf{\Pi}}^{\mathbf{l}}$,

$$\min_{z(k+1)} \left[g_v(z) + (\lambda(k))^T \left(\bar{\mathsf{v}}_j(k) - z_j(k)\right) + \frac{\rho}{2} \|\bar{\mathsf{v}}_j(k) - z_j(k)\|_2^2 \right]$$

7: Compute the stopping criteria $\forall k = 1, \ldots, H_p$

$$S_{c,1}(k) = \sum_{j=1}^{p} \varepsilon_{v_j} \mathsf{v}_j(k) - m_{M_i}(k)$$
$$S_{c,2}(k) = \mathsf{v}_j(k) - z_j(k)$$

8: Update the Lagrange multiplier

$$\lambda(k+1) = \lambda(k) + \rho \left(\bar{\mathsf{v}}_j(k) - \bar{z}_j(k) \right)$$

9: **until** $S_{c,1}(k) \leq \epsilon_1$ and $S_{c,2}(k) \leq \epsilon_2$ $\forall k$

10: Gather all optimal solutions for local controllers

11: Apply the first component of the optimal solution

12: Increase k to $k+1$ and repeat the procedure from step 1

the same no matter the selection of v_1 or v_3.

In addition, an extra weighting matrix I_{v_j} is required into the quadratic term of the consensus stage in (8b). This matrix is fixed in a way that it allows penalising the current capacity of the peripheral devices to provide resources without real-time energy conversion. The last fact is because if any process variable, e.g., pressure or the coolant level in the tanks, is near to its lower boundary and the controller decides to supply the required flow from this system, then the related peripheral device must be activated. Then, to determine I_{v_j}, based on the optimal solution of each local controller a prediction for the process dynamics is made, i.e., pressure dynamics for SS_1 and SS_2 and level dynamics for SS_3 and SS_4, and a vector of weights is created in the following way. At each instant k, for every time step r along H_p, the value of the process variable Q_j is normalised as $\hat{Q}_j(r) = (\, Q_j(r) - \underline{Q}_j \,)/(\, \overline{Q}_j - \underline{Q}_j \,)$.

Once the normalised value $\hat{Q}_j(r)$ is computed, the extra penalisation for selecting v_j according to the level of Q_j at each time step r is defined as $w_{Q_j}(r) = 1 + (1 - \hat{Q}_j(r))$. Thus, when Q_j is near $\underline{Q}_j$, the peripheral device and the valve related to this process dynamics will have a higher penalisation since if the associated valve v_j opens, then the peripheral device should be turned on early than if the resource is provided from another device. In contrast, if Q_j is close to $\overline{Q}_j$, the penalty for supplying resources from v_j will be less to promote the use of this device before other devices with less capacity. Thereby, the matrices I_{v_j} at the consensus stages are defined as $I_{v_j} = W_{Q_j} \left(10\, I_{H_p}\right)$, with W_{Q_j} the vector of w_{Q_j} along H_p at each time instant k, and I_{H_p} the identity matrix of suitable dimensions used to get the matrix structure.

Table 3: Comparison among centralised and non-centralised control architectures.

Controller	Energy consumption [VA]	Maximum S(k) [VA]
C-MPC	1973528.069	2344.263
Ad-NCDMPC	1973857.628	2376.881
Ad-CDMPC	1972556.607	2304.056

The results presented below correspond to both the non-cooperative and cooperative architectures, denoted as Ad-NCDMPC and Ad-CDMPC, and a centralised MPC (C-MPC) designed according to the case study. All simulations were performed during 30 machine cycles for the machine with the longest cycle time. The obtained results for the tested control strategies are summarised in Table 3, in which the total energy consumption is computed according to (2). Besides, the optimal activation/deactivation sequences for peripheral devices obtained from using both centralised and non-centralised control architectures are shown in Figures 7a and 7b, while the resulting energy consumption profile for the whole process line is presented in Figure 8. From the results in Table 3, it is possible to conclude that closed-loop performance similar to that obtained with centralized control approaches can be achieved using the proposed non-centralized control scheme. It means that the modularisation of control systems could be an appropriate way to promote the flexibility of manufacturing systems since, if the consensus stage between the subsystems is properly defined, the control objective can be achieved with a performance similar to that of the centralised case as shown in Figure 8.

Although the effectiveness of both the centralised and non-centralised control approaches is similar, their activation sequences are different, and the main differences refer to the activation sequence for the valve apertures as shown in Figures 9a and 9b. It should be noted that for the case of the supply system of compressed air, the optimal sequences obtained for both control architectures were the same, mainly since this system is more constrained that the coolant-supply system. However, for the supply system of coolant, in which more solutions for both v_2 and v_4 are allowed, the centralised control strategy decides to use both P_{G_2} and P_{G_3} to satisfy the coolant demand from M_3. Then, as a consequence of these differences, the activation sequences for peripheral devices were also different since the controller should keep trying to minimise the energy consumption and satisfying the process constraints according to the current status of the process line.

According to the literature about centralised and non-centralised control systems, the former are those that can achieve the optimal solution, and the non-centralised control

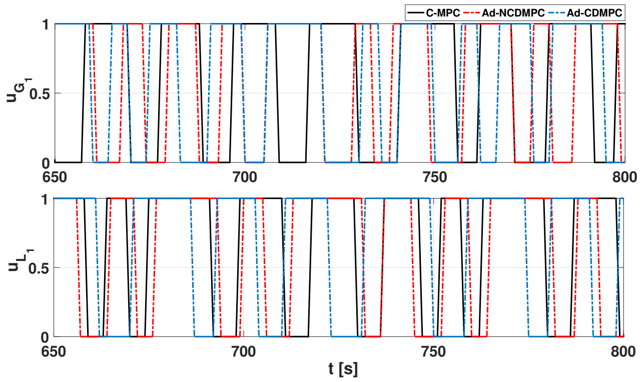

(a) Activation sequences for P_{G_1} and P_{L_1}.

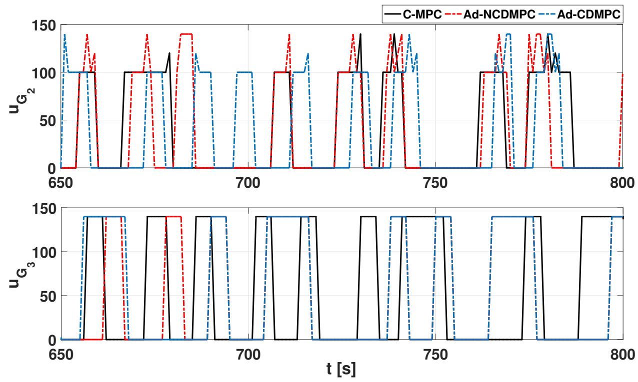

(b) Activation sequences for P_{G_2} and P_{G_3}.

Figure 7: Optimal activation sequences of peripheral devices by using centralised and non-centralised control architectures.

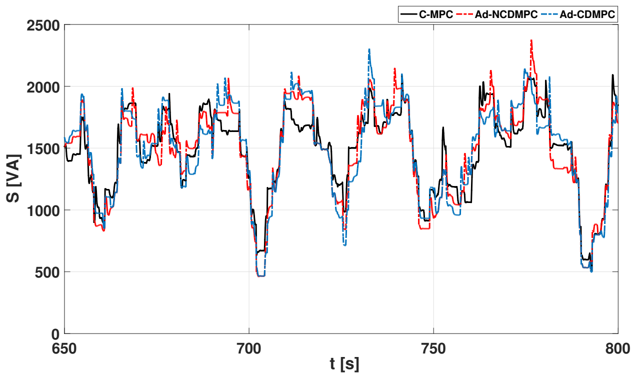

Figure 8: Energy consumption profile obtained by using centralised and non-centralised control architectures.

schemes could match the centralised behaviour if there exists cooperation among the local controllers. From the results in Table 3, it could be said that the non-centralised control strategies allow achieving better results. However, since the differences obtained among all the control strategies do not surpass 0.05%, it can be said that such differences are due to numerically issues more than related to the closed-loop performance of the control strategies. It means, due to the number of decision variables the centralised control approach should consider, the discrete and binary nature of such variables, and the resulting combinations, the solver selected cannot test all the possible solutions before to reach its predefined stopping criteria. In contrast, since the size of local controllers is significantly lower than the one in the centralised case, probably, every local controller can test all the possible solutions before reaching the stopping criteria of the solver, and choose the best one. From this fact, non-centralised control approaches could represent advantages regarding the centralised ones when the size of the systems increase.

In Figure 10, the CPU time spent by iteration for each one of the control strategies tested is shown. In this figure, the time spent to find an optimal solution for the centralised approach is compared with the time spent to achieve a solution by the slower set of coupled sub-systems in Ad-NCDMPC, and the time needed by Ad-CDMPC to find the optimal solution. Based on these results, both C-MPC and Ad-NCDMPC find an optimal solution faster than the Ad-CDMPC strategy, which requires more iterations to reach a consensus among all local controllers that satisfies the stopping criteria regarding the global cost function. Although the local controllers in the case of non-cooperative control architecture have lower dimension than in the centralised case, the time to find an optimal solution is quite similar for both architectures since the solution method employed (ADMM) is iterative, and the exchange of information among local controllers is required to get a consensus among them. However, even when each local controller for the non-cooperative case requires more than one iteration to the satisfy stopping criteria, the optimal solution was always found within a second. The last statement did not always hold for the centralised case, for which more than one second was sometimes required to find an optimal solution.

6. Conclusion

In this paper, a methodology for the design of non-centralised control architectures (both cooperative and non-cooperative) to improve the energy efficiency of manufacturing systems without affecting the system productivity is proposed. Thus, using the proposed approaches, control schemes could also be modularised to confer more flexibility to manufacturing systems. Moreover, due to the strongly coupled dynamics of such systems, algorithms based on ADMM were proposed to solve the local optimisation problems in a distributed way, including the energy consumption into the consensus stage. Regarding the energy consumption, the non-centralised architectures have a similar closed-loop performance with respect to the centralised counterpart. Although the cooperative case demands a higher computational burden, in the non-cooperative case the optimal solution was always found within a second, allowing such a strategy to be suitable for its implementation.

Finally, based on the proposed design and assumptions, both fixed and time-varying partitioning methodologies could be implemented to test the closed-loop performance of the proposed control strategy. Besides, non-iterative methods could be tested

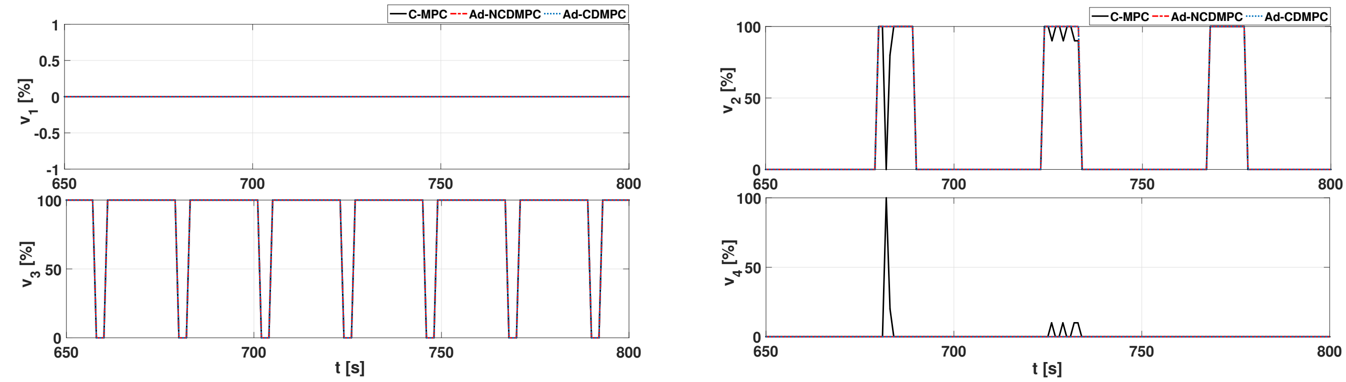

(a) Activation sequences for v_1 and v_3.

(b) Activation sequences for v_2 and v_4.

Figure 9: Optimal activation sequences for the aperture of valves by using centralised and non-centralised control architectures.

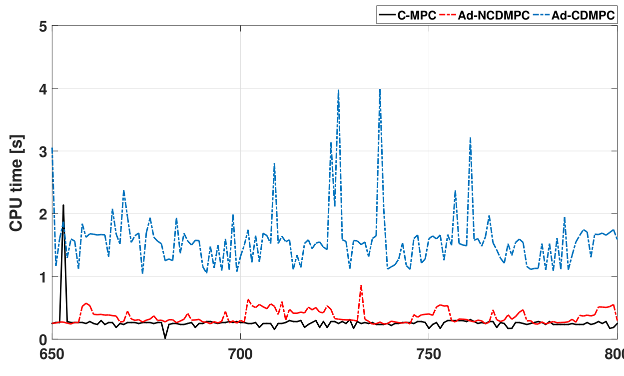

Figure 10: CPU time spent by iteration to find an optimal solution by using centralised and non-centralised control architectures.

to solve the optimisation problems in a distributed way, and also, feasibility and stability proofs should be performed to guarantee the convergence of the proposed controller.

Acknowledgements

This work has been funded by the FI-AGAUR scholarship of the Catalan government.

References

[1] H. ElMaraghy, T. AlGeddawy, A. Azab, W. ElMaraghy, Change in Manufacturing – Research and Industrial Challenges, Springer, Berlin, Heidelberg, 2012, pp. 2–9 (2012).

[2] J. L. Diaz C., C. Ocampo-Martinez, S. Olaru, Dual mode control strategy for the energy efficiency of complex and flexible manufacturing systems, Journal of Manufacturing Systems 56 (2020) 104–116 (2020). doi:doi.org/10.1016/j.jmsy.2020.05.009.

[3] Z. Cao, C. Lin, M. Zhou, A knowledge-based cuckoo search algorithm to schedule a flexible job shop with sequencing flexibility, IEEE Transactions on Automation Science and Engineering (2019) 1–14 (2019).

[4] C. Schultz, S. Braunreuther, G. Reinhart, Method for an energy-oriented production control, Procedia CIRP 48 (2016) 248–253, the 23rd CIRP Conference on Life Cycle Engineering (2016). doi:10.1016/j.procir.2016.04.058.

[5] C. Yan, Z. Zheng, Problem formulation and solution methodology for energy consumption optimization in bernoulli serial lines, IEEE Transactions on Automation Science and Engineering (2020) 1–15 (2020).

[6] J. L. Diaz C., M. Bermeo, J. Diaz-Rozo, C. Ocampo-Martinez, An optimization-based control strategy for energy efficiency of discrete manufacturing systems, ISA Transactions 93 (2019) 399 – 409 (2019).

[7] J. M. Maestre, R. R. Negenborn, Distributed model predictive control made easy, Springer, Dordrecht, 2014 (2014).

[8] F. Tedesco, C. Ocampo-Martinez, A. Casavola, V. Puig, Centralized and distributed command governor approaches for water supply systems management, IEEE Transactions on Systems, Man, and Cybernetics: Systems 48 (4) (2018) 586–595 (2018). doi:10.1109/TSMC.2016.2612361.

[9] P. A. Trodden, J. M. Maestre, Distributed predictive control with minimization of mutual disturbances, Automatica 77 (2017) 31–43 (2017). doi:10.1016/j.automatica.2016.11.023.

[10] G. Franzè, W. Lucia, F. Tedesco, A distributed model predictive control scheme for leader–follower multi-agent systems, International Journal of Control 91 (2) (2018) 369–382 (2018). doi:10.1080/00207179.2017.1282178.

[11] M. Dornhöfer, S. Sack, J. Zenkert, M. Fathi, Simulation of smart factory processes applying multi-agent-systems—a knowledge management perspective, Journal of Manufacturing and Materials Processing 4 (3) (2020) 89 (Sep 2020). doi:10.3390/jmmp4030089.
URL `http://dx.doi.org/10.3390/jmmp4030089`

[12] J. Barreiro-Gomez, C. Ocampo-Martinez, N. Quijano, Time-varying partitioning for predictive control design: Density-games approach, Journal of Process Control 75 (2019) 1 – 14 (2019). doi:10.1016/j.jprocont.2018.12.011.

[13] W. D. Li, L. Gao, X. Y. Li, Y. Guo, Game theory-based cooperation of process planning and scheduling, in: 2008 12th International Conference on Computer Supported Cooperative Work in Design, 2008, pp. 841–845 (2008). doi:10.1109/CSCWD.2008.4537088.

[14] Y. G. Kim, S. Lee, J. Son, H. Bae, B. D. Chung, Multi-agent system and reinforcement learning approach for distributed intelligence in a flexible smart manufacturing system, Journal of Manufacturing Systems 57 (2020) 440–450 (2020). doi:doi.org/10.1016/j.jmsy.2020.11.004.

[15] E. S. Okpoti, I.-J. Jeong, A reactive decentralized coordination algorithm for event-driven production planning and control: A cyber-physical production system prototype case study, Journal of Manufacturing Systems 58 (2021) 143–158 (2021). doi:doi.org/10.1016/j.jmsy.2020.11.002.

[16] M. E. Leusin, M. Kück, E. M. Frazzon, M. U. Maldonado, M. Freitag, Potential of a multi-agent system approach for production control in smart factories, IFAC-PapersOnLine 51 (11) (2018) 1459 – 1464, 16th IFAC Symposium on Information Control Problems in Manufacturing INCOM 2018 (2018). doi:10.1016/j.ifacol.2018.08.309.

[17] J. Du, P. Dong, V. Sugumaran, D. Castro-Lacouture, Dynamic decision support framework for production scheduling using a combined genetic algorithm and multiagent model, Expert Systems 38 (1) (Feb. 2020). doi:10.1111/exsy.12533.

[18] Y. Zhang, J. Wang, S. Liu, C. Qian, Game theory based real-time shop

floor scheduling strategy and method for cloud manufacturing, International Journal of Intelligent Systems 32 (4) (2016) 437–463 (Nov. 2016). doi:10.1002/int.21868.
[19] J. L. Diaz C., C. Ocampo-Martinez, Energy efficiency in discrete-manufacturing systems: Insights, trends, and control strategies, Journal of Manufacturing Systems 52 (2019) 131–145 (2019). doi:doi.org/10.1016/j.jmsy.2019.05.002.
[20] P. D. Christofides, R. Scattolini, D. M. D. la Peña, J. Liu, Distributed model predictive control: A tutorial review and future research directions, Computers & Chemical Engineering 51 (Supplement C) (2013) 21–41 (2013). doi:10.1016/j.compchemeng.2012.05.011.
[21] R. Scattolini, Architectures for distributed and hierarchical model predictive control – A review, Journal of Process Control 19 (5) (2009) 723–731 (2009). doi:10.1016/j.jprocont.2009.02.003.
[22] S. Boyd, Distributed optimization and statistical learning via the alternating direction method of multipliers, Foundations and Trends in Machine Learning 3 (1) (2010) 1–122 (2010). doi:10.1561/2200000016.
[23] P. Giselsson, A. Rantzer, Distributed model predictive control with suboptimality and stability guarantees, in: 49th IEEE Conference on Decision and Control (CDC), 2010, pp. 7272–7277 (Dec 2010). doi:10.1109/CDC.2010.5717026.
[24] B. Biegel, J. Stoustrup, P. Andersen, Distributed MPC via dual decomposition, in: Distributed Model Predictive Control Made Easy, Springer Netherlands, 2013, pp. 179–192 (2013). doi:10.1007/978-94-007-7006-5-11.
[25] F. Lin, M. Fardad, M. R. Jovanović, Design of optimal sparse feedback gains via the alternating direction method of multipliers, IEEE Transactions on Automatic Control 58 (9) (2013) 2426–2431 (2013). doi:10.1109/TAC.2013.2257618.
[26] S. Lee, N. Chatzipanagiotis, M. M. Zavlanos, Complexity certification of a distributed augmented lagrangian method, IEEE Transactions on Automatic Control 63 (3) (2018) 827–834 (2018). doi:10.1109/TAC.2017.2747503.
[27] Y. Zhang, M. M. Zavlanos, A consensus-based distributed augmented Lagrangian method, in: 2018 IEEE Conference on Decision and Control (CDC), 2018, pp. 1763–1768 (Dec 2018). doi:10.1109/CDC.2018.8619512.
[28] C. Papadopoulos, J. Li, M. O'Kelly, A classification and review of timed Markov models of manufacturing systems, Computers & Industrial Engineering 128 (2019) 219–244 (2019). doi:10.1016/j.cie.2018.12.019.
[29] S. Qin, An overview of subspace identification, Computers & Chemical Engineering 30 (10) (2006) 1502–1513 (2006). doi:10.1016/j.compchemeng.2006.05.045.
[30] P. Overschee, B. De Moor, Subspace Identification for Linear Systems: Theory - Implementation - Applications, Springer US, Boston, MA, 1996 (1996).
[31] IBM, IBM ILOG CPLEX optimization studio, v 12.5 (2013).
[32] J. Löfberg, Yalmip : A toolbox for modeling and optimization in Matlab, in: In Proceedings of the CACSD Conference, Taipei, Taiwan, 2004 (2004).